RSC Advances

ROYAL SOCIETY OF CHEMISTRY

www.rsc.org/advances

Journal Name

ARTICLE

Controlled synthesis of the monoclinic and orthorhombic polymorphs of Sr_2SiO_4 activated with Ce^{3+} or Eu^{2+}

Received 00th January 20xx,
Accepted 00th January 20xx

DOI: 10.1039/x0xx00000x

www.rsc.org/

A. Madej,[a] E. Zych [a,b] †

Phase pure orthorhombic and monoclinic Sr_2SiO_4 and its Ce^{3+}- or Eu^{2+}-activated versions were synthesized using H_3BO_3 or $SrCl_2$ fluxes. The effects of the type of the dopant and its concentration as well as the type of flux on the crystallization were revealed and discussed. The luminescent properties of the phase pure Ce^{3+} or Eu^{2+} activated powders were characterized both at 30 K and 300 K. The presence of two luminescent sites was proved in both types of structures and in the case of both activators and their characteristic excitation and emission spectra were presented. Energy transfer from ions emitting at higher-energies to those giving luminescence at lower energies was showed to take place in both polymorphs and in the case of each of the dopants. Eu^{2+} emissions of both sites in both structures locate fully in the visible part of spectrum, while part of Ce^{3+} luminescence occurs in long-wavelength UV. Room temperature radioluminescence spectra showed that only the site emitting at longer wavelengths, in both structures and for both dopants, is active in the scintillation process. For the first time, for both dopants luminescence from the two sites in both polymorphs of Sr_2SrO_4 are spectroscopically characterized at 30 K and room temperature.

Introduction

Properly activated silicates were recognized as efficient luminescent materials. They found applications as scintillators or phosphors for lighting, recently for white LEDs [1-26]. This is the last application, solid state lighting (SSL), which boosted research on Sr_2SiO_4 in recent years, as activation of this host with Eu^{2+} or Ce^{3+} seemed to lead to luminescence useful in this field of technology [1-5, 10-19, 24-26].

It is already about thirty years as first reports on crystal structure of Sr_2SiO_4 were published by Catti and his co-workers [27-30]. Existence of two polymorphs, orthorhombic α'-Sr_2SiO_4 and monoclinic β-Sr_2SiO_4, together with some data on their phase transitions were then presented.

The orthorhombic α'-form crystallizes in the Pmnb space group, while the monoclinic β-form in the $P12_1/n_1$ space group. Most of the studies proved that getting phase-pure Sr_2SiO_4, unlopped or activated, is a difficult task and till now there are not known clear rules managing the phase equilibrium in Sr_2SiO_4. For example, replacing some Sr^{2+} ions with either larger Ba^{2+} or smaller Ca^{2+} seemed to stabilize the orthorhombic structure [1, 14, 23, 29, 30]. It was suggested that the stabilization is due to changes in the lengths of metal-oxygen bonds [1,5,14,16,23,29,30].

Consequently, in most of the published papers on luminescent properties of Sr_2SiO_4-based phosphors mixtures of both phases were obtained and investigated [4,5,12,14,25]. Nevertheless, it was reported that pure orthorhombic [13,15-20,22,24,26] or monoclinic phases [9,11,18,21] could be synthesized when Sr_2SiO_4 was doped with Eu^{2+}, Eu^{3+}, Dy^{3+} or Tb^{3+} ions. Thus, it appeared that just a small amount of the impurity ions was able to stabilize one of the two structures. It was indicated that getting the orthorhombic α'-form is possible when more than 1 mol% of dopants having ionic radii similar to Sr^{2+} ion are used. In fact, the problem of getting phase-pure powders was so difficult to solve that products with only a residual impurity phase were sometimes claimed to be phase-pure. A close examination of presented XRD patterns proves, however, the presence of a small amount of the other polymorph [1,2,6,8,10,23,25].

The two structures, orthorhombic α'-Sr_2SiO_4 and monoclinic β-Sr_2SiO_4, present some similarities important for spectroscopic properties of the incorporated activators. First, in each of them Sr^{2+} ions occupy two different symmetry sites. Second, the coordination numbers (CN) of the metal sites in both phases are the same: CN=10 (Sr(1)) and CN=9 (Sr(2)). In Fig. 1 we present unit cells of both structures together with the local arrangements of the two Sr sites in each of them. In Table 1 we list the Sr-O and Sr-Sr distances in the orthorhombic α'-Sr_2SiO_4 and monoclinic β-Sr_2SiO_4 which might be helpful in understanding the spectroscopic properties of these compositions when doped with Ce^{3+} or Eu^{2+} ions. Let us yet

[a] Faculty of Chemistry, University of Wroclaw, 14 F. Joliot-Curie Street, 50-383 Wroclaw, Poland
[b] Wroclaw Research Centre EIT+, 147 Stablowicka Street, 54-066 Wroclaw, Poland
† corresponding author: Eugeniusz Zych e-mail:Eugeniusz.zych@chem.uni.wroc.pl
Electronic Supplementary Information (ESI) available: [details of any supplementary information available should be included here]. See DOI: 10.1039/x0xx00000x

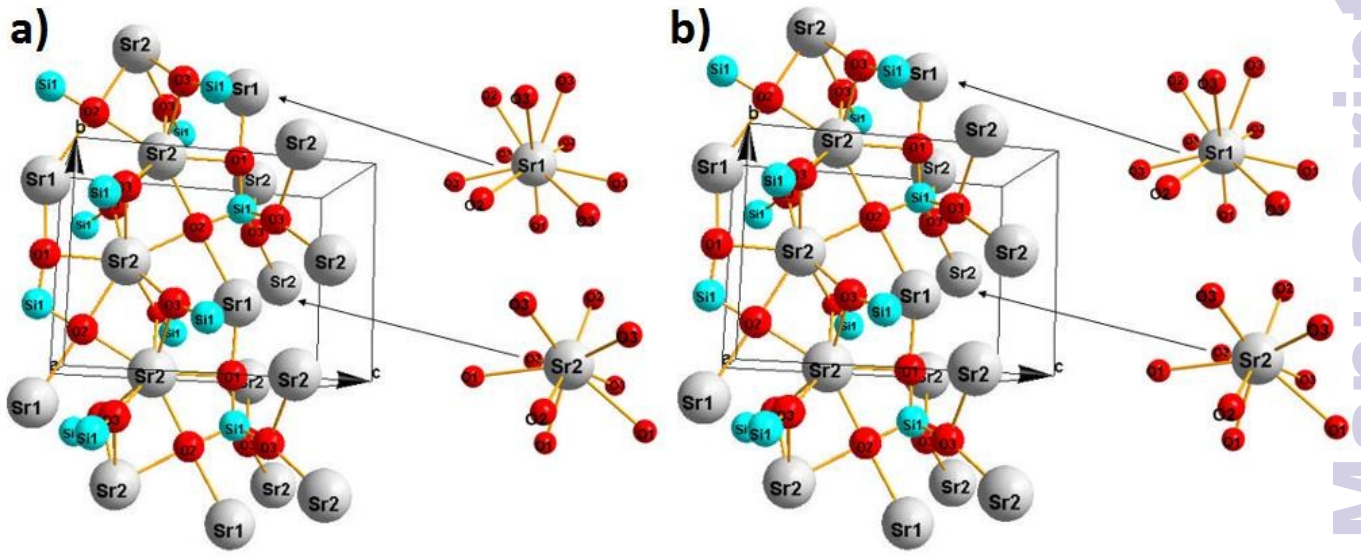

Fig.1. Unit cells of both structures a)orthorhombic and b) monoclinic- Sr_2SiO_4 together with the local arrangements of the two Sr sites in each of them.

note, that both the shortest and average Sr(1)-O and Sr(2)-O distances in the two structures are similar. This, combined with identical CNs, may justify quite similar energetic positions of at least the lowest (emitting) 5d levels of Ce^{3+} or Eu^{2+} dopants occupying analogous - (Sr(1) or Sr(2)) - sites in the two polymorphs. Yet, since the 5d orbitals are the most outside located and are not screened from the influence of the surrounding, even the small changes in the distances should exert measureable effects on the orbitals energetic positions. In contrary, when we compare the shortest and average distances, of Sr(1)-O and Sr(2)-O within the same polymorph, we see that they differ quite significantly (see Table 1). Thus we can expect that within the same structure, both in the case of Ce^{3+} and Eu^{2+}, the energetic position of the emitting states should differ quite profoundly. The Sr(1)-Sr(2) distances are short, which obviously favours energy exchange between dopants occupying different sites in either of the two hosts. We shall see that such energy transfer is indeed efficient in both hosts and for both activators. In this paper we shall show that it is possible to synthesize phase pure Sr_2SiO_4:Ce and Sr_2SiO_4:Eu (both orthorhombic and monoclinic) phosphors using two different fluxes, $SrCl_2$ and H_3BO_3. It will be proved that applying H_3BO_3 and using any of the dopants, Ce or Eu, the powders crystallize in the orthorhombic α'-phase. However, $SrCl_2$ flux leads to the monoclinic β-phase in the case of Sr_2SiO_4:Ce powders or when not more than 0.1 mol% of Eu was doped. On the other hand using 1 mol% of Eu causes crystallization in the orthorhombic α'-phase. Photo- and radioluminescent properties of the phase pure phosphors in the 30-300 K range of temperatures will also be presented.

Experimental details

Synthesis and structural characterization

All of the strontium silicate powders, undoped and Ce- or Eu-doped, were prepared by flux-aided synthesis. As the flux either $SrCl_2$ or H_3BO_3 were used. The starting materials were $SrCO_3$ (99.994%, Alfa Aesar), SiO_2 (99%, Sigma Aldrich), CeO_2 (99.99% Stanford Materials Corporation) or Eu_2O_3 (99.999%, Stanford Materials Corporation). 1 wt.% of H_3BO_3 (99.8% Carl Roth GmbH+Co) was added to the reacting mixture, while in the case of $SrCl_2$ flux (99%, Merck, hydrated salt, $SrCl_2 \bullet 6H_2O$, was used) it was 1, 5, 10, 15 or 50 wt.%. The stoichiometric amounts of substrates were mixed with an appropriate flux, thoroughly ground in an alumina mortar and were heat-treated afterwards for 4 hours in different atmospheres (air, vacuum, active carbon with reduced access of air, forming gas (H_2(5%)/N_2(95%), or H_2(25%)/N_2(75%)) at various temperatures between 1200-1400°C. Powders after reaction with $SrCl_2$ were recovered by washing out the flux with hot deionized water. In the case of Eu-doped samples obtained by heating in the presence of active carbon additional heating at 650°C for 0.5h in air was undertaken to remove carbon residues. All the most important data on the synthesis parameters of specific samples are collected in Table 2 together with the information on the phase composition of the products as revealed by recorded XRD patterns.

To monitor completeness of the reaction and phase purity of the products, X-ray diffraction (XRD) patterns were measured with a Brucker D8 Advance diffractometer equipped with a Cu lamp. The measurements were taken in the range of 2θ = 10-90° with 2θ = 0.032° steps.

The morphology of the powders was revealed by means of scanning electron microscopy (SEM) imaging with Hitachi S-3400N equipped with an energy dispersive X-ray spectroscopy (EDX) EDAX analyser.

Table 1. The Sr-O and Sr-Sr distances in the orthorhombic α'-Sr_2SiO_4 and monoclinic β-Sr_2SiO_4.

	α'-Sr_2SiO_4	β-Sr_2SiO_4
Sr(1)-O (1^{I})	2.386(7)	2.37(1)
Sr(1)-O (2)	2.771(7)	2.801(8)
Sr(1)-O (2,2^{III})	2.842(6) (x2)	2.57(1)
Sr(1)-O (2,2^{II})		3.11(1)
Sr(1)-O (3)	3.021(6) (x2)	2.764(8)
Sr(1)-O (4)		3.199(8)
Sr(1)-O (3,2^{II})	2.846(6) (x2)	2.63(1)
Sr(1)-O (4,2^{II})		2.93(1)
Sr(1)-O (3,4^{V})	2.972(7) (x2)	3.35(1)
Sr(1)-O (4,4^{V})		2.78(1)
Average	2.852	2.850
Sr(2)-O (1^{I})	2.593(8)	2.62(1)
Sr(2)-O (2^{I})	2.622(7)	2.651(8)
Sr(2)-O (2,4^{I})	2.622(7)	2.624(9)
Sr(2)-O (1,2^{III})	3.105(3) (x2)	3.40(1)
Sr(2)-O (1,2^{II})		2.78(1)
Sr(2)-O (3,2^{II})	2.609(6) (x2)	2.694(8)
Sr(2)-O (4,2^{III})		2.565(8)
Sr(2)-O (3,3^{VI})	2.507(6) (x2)	2.527(9)
Sr(2)-O (4,3^{VIII})		2.519(9)
Average	2.698	2.709
Sr(1)-Sr(1)	3.019	4.891
	3.796	5.683
	3.951	3.866
	4.867	3.957
	5.811	5.851
	5.796	
Sr(1)-Sr(2)	3.897	3.705
	3.634	3.622
	3.894	3.746
	3.757	4.083
		3.874
Sr(2)-Sr(2)	3.689	3.690
	4.799	4.558
	5.682	5.663

Optical spectroscopy

Photoluminescence and excitation spectra were recorded using an FLS980-sm Fluorescence Spectrometer from Edinburgh Instruments Ltd. using a 450 W continuous Xenon arc lamp for excitation and equipped with a closed-cycle helium cryostat ARS-4HW from Advanced Research System, Inc. Both excitation and emission monochromators were of single grating Czerny-Turner type, with 300 mm focal length. A pellet of a studied powder, some 7 mm in diameter, was formed under a force of 2-3 tones. It was then mounted on a cold finger of a cryostat and transferred to the sample chamber of the spectrometer. Hamamatsu R928P high-gain photomultiplier detector was used to record the luminescence light. Emission spectra were corrected for the recording system efficiency and excitation spectra were corrected for the incident light intensity. These measurements were taken in the range of 30-300 K.

Room temperature radioluminescence (RL) spectra were recorded using white X-rays from a Cu X-ray tube working under the voltage of 40 kV and the current of 10 mA. The emission photons were collected with a 74-UV lens connected to a QP600-2-SR-BX waveguide which transferred the luminescent light to an Ocean Optics HR2000CG-UV-NIR Spectrometer controlled by a dedicated SpectraSuit software. The RL light yields of our materials were compared with the results for Lu_2SiO_5:Ce (LSO) commercial powder kindly offered by Phosphor Technology Ltd.

Results and discussion

XRD measurements

Fig. 2 presents exemplary XRD patterns of Sr_2SiO_4 (Fig. 2a), Sr_2SiO_4:Ce (Fig. 2b-sample SCe15, SCe23, SCe26) and Sr_2SiO_4:Eu (Fig. 2c- sample SEu1, SEu8, SEu12) prepared at 1400°C for 4h using $SrCl_2$ (different amounts related to the phosphor) or H_3BO_3 flux. A summary of observations on the resultant phosphors phase composition are given in Table 2. Upon the XRD data the following conclusions about the products crystal structure could be derived:

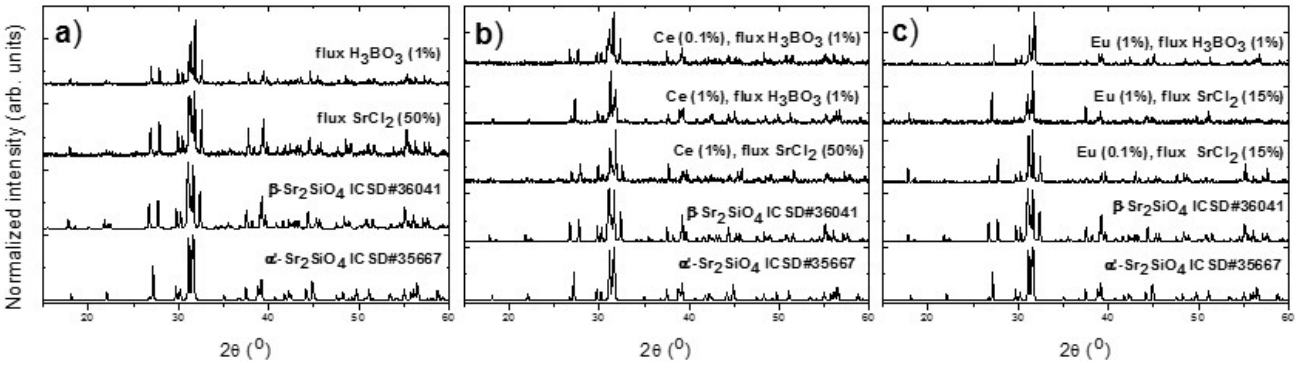

Fig.2. XRD pattern of Sr_2SiO_4 powders: a) undoped, b) Ce-doped (SCe15, SCe23, SCe26), c) Eu-doped (SEu1, SEu8, SEu12) obtained in the synthesis at 1400°C for 4h with fluxes $SrCl_2$ and H_3BO_3.

I. Undoped Sr_2SiO_4 powders obtained in synthesis with either $SrCl_2$ or H_3BO_3 flux crystallizes in monoclinic system (see Fig. 2a).

II. Sr_2SiO_4:Ce obtained using more than 10 wt.% of $SrCl_2$ flux crystallizes in monoclinic structure. Lower content of the flux leads to a mixture of α'- and β-phases.

III. Sr_2SiO_4:Ce obtained using H_3BO_3 flux tends to crystallize in orthorhombic structure but phase pure powder is formed only when the Ce content is not lower than 1 mol% (with respect to Sr) and the preparation temperature is not lower than 1300 °C. Processing below 1300 °C and/or using less than 1 mol% of Ce leads to a powder composed of a mixture of both phases.

IV. Sr_2SiO_4 doped with 0.1 mol% Eu synthesized with the $SrCl_2$ flux crystallizes in monoclinic structure, while 0.5 mol% concentration of Eu leads to a mixture of α'- and β-phases. Yet, higher concentrations gives orthorhombic structure.

V. Powders containing 0.1 mol% of Eu and made with H_3BO_3 flux contain mixture of both phases.

VI. Sr_2SiO_4:Eu powders crystallize in purely orthorhombic phase when the Eu content is not lower than 1 mol% regardless whether $SrCl_2$ or H_3BO_3 flux is used.

Table 2. Processing parameters of selected samples and structural composition of the products.

Processing parameters				**Sr_2SiO_4:Ce**		
Temperature	**Time**	**Atmosphere**	**Flux (wt%)**	**Dopant Concentration (mol%)**	**Structure of the product**	**Composition number**
1200°C	4h	air	1%, 5%, 10% $SrCl_2$	1%	mixture of both phases	SCe1, SCe4, SCe7
			15%, 50% $SrCl_2$	1%	monoclinic	SCe10, SCe13
			50% $SrCl_2$	0.1%	monoclinic	SCe17
			1% H_3BO_3	0.1%, 1%, 1.5%	mixture of both phases	SCe21, SCe24, SCe27
1300°C	4h	air	1%, 5%, 10% $SrCl_2$	1%	mixture of both phases	SCe2, SCe5, SCe8
			15% $SrCl_2$	1%	monoclinic	SCe11
			50% $SrCl_2$	0.1%	monoclinic	SCe18
			1% H_3BO_3	0.1%	mixture of both phases	SCe22
			1% H_3BO_3	1%, 1.5%	orthorhombic	SCe25, SCe28
1300°C + cooling to 850°C 3°C/min	4h	air	50% $SrCl_2$	0.1%, 1%	monoclinic	SCe19, SCe14
1400°C	4h	air	1%, 5%, 10% $SrCl_2$	1%	mixture of both phases	SCe3, SCe6, SCe9
			15%, 50% $SrCl_2$	1%	monoclinic	SCe12, SCe15
			50% $SrCl_2$	0.1%	monoclinic	SCe20
			1% H_3BO_3	0.1%	mixture of both phases	SCe23
			1% H_3BO_3	1%, 1.5%	orthorhombic	SCe26, SCe29
1400°C + cooling to 850°C 3°C/min	4h	air	15% $SrCl_2$	1%	monoclinic	SCe16
				Sr_2SiO_4:Eu		
1300°C	4h	air	15% $SrCl_2$	1%	orthorhombic	SEu3
1400°C	4h	air	15% $SrCl_2$	1%	orthorhombic	SEu4
			1% H_3BO_3	1%	orthorhombic	SEu11
1400°C	4h	active carbon	15% $SrCl_2$	1%	orthorhombic	SEu7
1) 1400°C 2) 1400°C	4h	air H_2(5%)/N_2(95%) H_2(25%)/N_2(75%)	15% $SrCl_2$	1%	orthorhombic	SEu5 SEu6
1) 1400°C 2) 650°C	4h 0.5h	active carbon air	15% $SrCl_2$	0.1%	monoclinic	SEu1
				0.5%	mixture of both phases	SEu2
				1%, 2%	orthorhombic	SEu8, SEu9
			1% H_3BO_3	0.1%	mixture of both phases	SEu10
				1%	orthorhombic	SEu12

Thus, using the two fluxes, Ce-activated Sr_2SiO_4 may be crystallized as phase-pure, either orthorhombic or monoclinic, phosphor. When Eu is used as the dopant, both phases can be obtained but crystallization depends on Eu concentration.

Morphology

Morphology of the products was strongly dependent on the flux used in the synthesis and, to some extent, parameters of the processing, especially the cooling rate. It was practically independent on the dopant. Exemplary, representative SEM images are presented in Figs. 3 and 4. In the presence of $SrCl_2$ flux, Sr_2SiO_4:Ce crystallized in monoclinic phase, as we already discussed. Its particles, see Fig. 3a (sample SCe15), were generally very large reaching about 30-40 µm. Yet, a fraction of the powder consisted of much smaller grains, on the order of a few microns. The small-grains portion was noticeably lowered if the cooling of the batch from 1400 °C to about 850 °C was not natural (faster) but controlled at the rate of 3 °C/min. This effect is presented in Fig. 3b (sample SCe16). It thus appears that the smaller particles were grown during the cooling from the product, presumably from the fraction dissolved in the $SrCl_2$ flux. Apparently, during faster cooling this portion crystallized giving finer particles, while the slow, controlled cooling allowed also the dissolved portion to crystallize into larger grains, at least partially. In the presence of H_3BO_3 flux (Fig. 3c- sample SCe26), when the orthorhombic phase of Sr_2SiO_4:Ce was formed, the grains were also relatively large with sizes ranging over 3-30 µm, roughly. Yet, they were rather irregular in shape and mostly not monocrystalline, but they consist of aggregates of smaller particles.

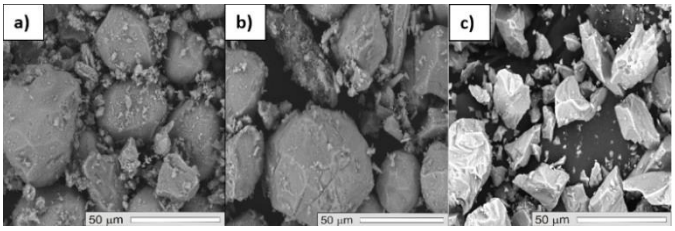

Fig.3. Morphology of Sr_2SiO_4:Ce(1 mol%) prepared at a)1400°C 4h with 50 wt% $SrCl_2$ (SCe15) b) 1400°C 4h with controlled cooling of 3 °C/min and 50 wt% of $SrCl_2$ flux (SCe16) – both crystallize in monoclinic phase c) 1400°C 4h with 1 wt% H_3BO_3 (SCe26)- crystallize in orthorhombic phase.

Sr_2SiO_4:1mol%Eu crystallized in the orthorhombic phase independently on the flux used in the synthesis. Yet, the morphology differed in both cases, as is presented in Fig. 4. Synthesis using $SrCl_2$ flux gave slightly elongated grains reaching the sizes of about 30x50 µm, see Fig. 4a. H_3BO_3 flux led to powders with much less uniform morphology, very similar to what was presented in Fig. 3c for the Ce-activated orthorhombic phase. Hence, it appears that the morphology of Sr_2SiO_4 is defined by the flux used in the synthesis and is actually hardly affected by the type of structure in which the powder crystallizes. The monoclinic Sr_2SiO_4:Ce (Fig. 3a,b) and orthorhombic Sr_2SiO_4:Eu powders (Fig. 4a) consist of particles

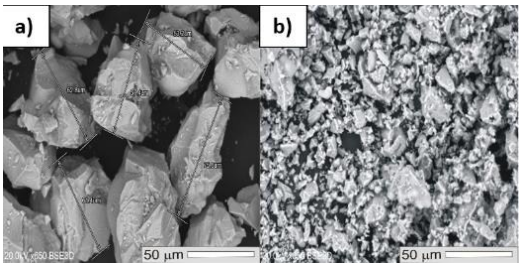

Fig.4. Morphology of Sr_2SiO_4:Eu (1 mol%) (orthorhombic phase) prepared at 1400°C 4h in the synthesis with a) 15 wt% $SrCl_2$ (SEu8) b) 1 wt% H_3BO_3 (SEu12).

quite similar in shape and sizes, although for the latter the small-grains fraction is practically absent even if the cooling rate was not controlled.

Photoluminescence of Sr_2SiO_4:Ce

Fig. 5 presents room temperature (RT) excitation and emission spectra of the orthorhombic –sample SCe26 (Fig. 5a,b) - and monoclinic - sample SCe15 (Fig. 5c,d) – phases of Sr_2SiO_4:1 mol% Ce powders. In both cases the luminescence locates in deep violet and blue part of spectrum. The orthorhombic α'-phase luminescence peaks around 410 nm and the monoclinic β-phase emission maximum appears around 400 nm. Clearly, at RT both the monoclinic and the orthorhombic structures produce very similar emission spectra. Thus, even having a mixture of the two phases the PL emission would be affected only slightly in terms of its spectral distribution (colour). The excitation bands consist of numerous bands in the case of both structures indicating a low symmetry of the luminescent centre, which is consistent with the structural properties of the polymorphs as presented in Fig. 1. As discussed in Introduction, in both structures Sr^{2+} occupies two different symmetry sites, and this should presumably also apply to the Ce^{3+} dopant. Yet, observed shifts

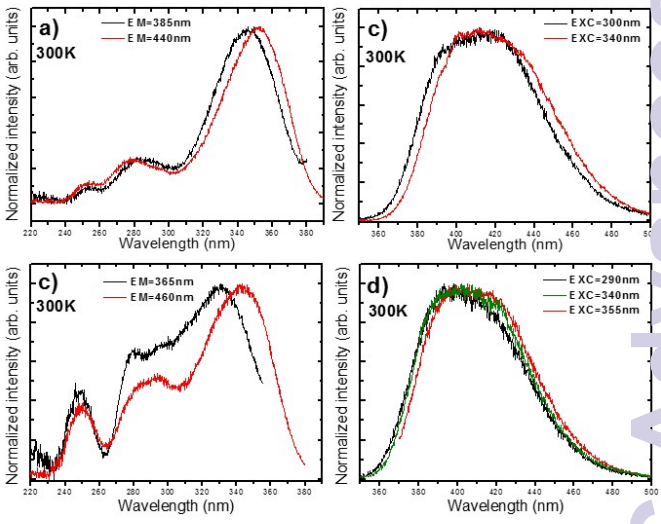

Fig.5. Excitation and emission spectra measured at RT for Sr_2SiO_4:1 mol% Ce powders obtained in the synthesis with fluxes: a) and b) 1 wt% H_3BO_3 orthorhombic phase (SCe26) , c) and d) 50 wt% $SrCl_2$ -monoclinic phase (SCe15)

of excitation bands positions depending on the monitored emission wavelength are only very small and similarly insignificant are changes in positions of the emissions excited at different wavelengths. Thus, at room temperature the spectra did not clearly prove that Ce occupies different symmetry sites. A similar set of experiments at low temperatures will verify this observation.

Nevertheless, at room temperature the emission bands of the orthorhombic Sr_2SiO_4: 1 mol% Ce (Fig. 5a,b) appear at wavelengths longer by about 5-10 nm and similar red shift is seen in the position of the lowest-energy excitation bands compared to the monoclinic phase. Bearing in mind that the average Sr-O distances in both structures are indeed very similar, see Table 1, the very small difference in the RT luminescence band positions is quite realistic, in fact.

Low temperature PL and PLE spectra of both phases of Sr_2SiO_4:Ce are presented in Fig. 6. Results related to the orthorhombic α'-phase are given in Fig. 6a,b (sample SCe26) and those connected with the monoclinic β-phase are presented in Fig. 6c,d (sample SCe15). Compared to the analogous RT spectra the presence of two Ce^{3+} emitting centres is now evident in both phases, while analogous RT spectra did not give a clear answer to that question (see Fig. 5). Comparison of the RT and low temperature results make it apparent that Ce(Sr1)→Ce(Sr2) energy transfer occurs even at 30 K. It is thus not surprising that at RT almost all emitted radiation comes from the Ce(Sr2) centre in both phases. In either of the two phases the PLE spectra of the long-wavelength emissions (Ce(Sr2)) the bands characteristic for the Ce(Sr1) centre emitting at shorter wavelengths are obviously present confirming the Ce(Sr1)→Ce(Sr2) energy transfer. At RT PLE spectra this effect was more profound, as expected. This is most clearly seen around 310 and 335 nm for the orthorhombic α'-phase (Fig. 6a) and around 310 nm for the monoclinic β-phase (Fig. 6c). Accordingly, appropriately selected excitation wavelengths allowed to separate the site-characteristic luminescent bands pretty fairly only at low temperature. This was more successful in the case of the monoclinic β-phase (Fig. 6d) than for the orthorhombic α'-phase (Fig. 6b). Altogether, according to the data presented in Fig. 6, the presence of two Ce^{3+} emitting centres is obvious in both structures. On the other hand, since positions of electronic levels of Ce(Sr1) and Ce(Sr2) centres favour energy transfer by the Förster mechanism [32] (which is proved by excitation spectra) it is not surprising that a complete spectroscopic separation of the site-related emission and excitation bands was not achieved.

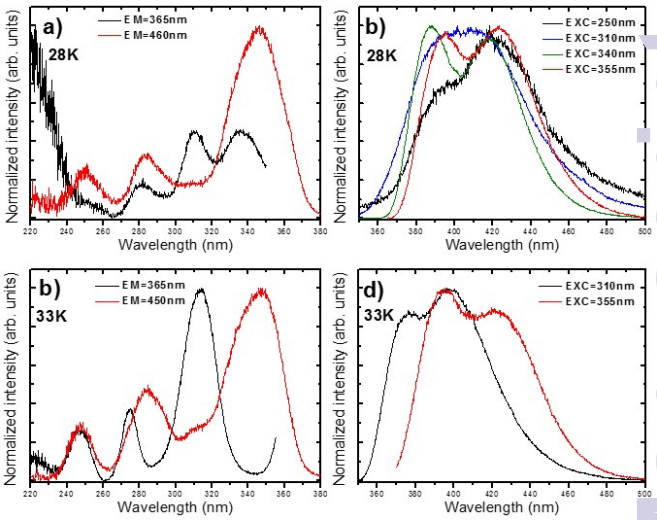

Fig.6. Excitation and emission spectra measured at low temperature for Sr_2SiO_4:1 mol% Ce powders obtained in the synthesis with fluxes: a) and b) 1 wt% H_3BO_3 orthorhombic phase (SCe26), c) and d) 50 wt% $SrCl_2$ -monoclinic phase (SCe15).

Photoluminescence of Sr_2SiO_4:Eu

Excitation and emission spectra of the orthorhombic Sr_2SiO_4:1mol%Eu are presented in Fig.7a,b (sample SEu8) and of the monoclinic phase in Fig. 7c,d (0.1mol%, sample SEu1). Regardless the crystallographic phase, for the Eu-activated composition it is evident already at RT that the dopant occupies at least two distinct symmetry sites with significantly different positions of the emitting and excitation bands. Excitation around 450 nm give rise to a characteristic broad-band luminescence peaking around 590 nm and 550 nm for α' and β-form, respectively (see Fig. 7b,d).In the case of orthorhombic α'-phase excitation around 290-330 nm produces a structured luminescent band in which the 590 nm component is accompanied by another, more energetic emission peaking around 480-500 nm (Fig. 7b). The latter component is less significant in intensity most probably due to anticipated Eu(Sr1)→Eu(Sr2) energy transfer. A greater change with excitation wavelength we observe in powders which crystallizes in the monoclinic β-phase. Excitation around 275-330 nm produces emission band with maximum around 470 nm accompanied with a component with maximum around 540-550 nm. Excitation at 250 nm favours luminescence peaking around 540 nm and upon 450 nm radiation exclusively this latter band is observed (Fig. 7d).

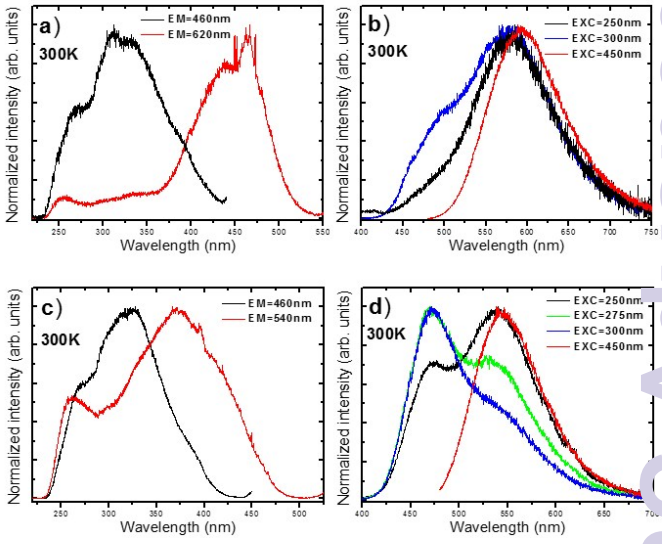

Fig.7. RT excitation and emission spectra of powders : a) and b) orthorhombic Sr_2SiO_4: 1mol% Eu (SEu8), c) and d) monoclinic- Sr_2SiO_4: 0.1 mol% Eu (SEu1).

Comparing the emission spectra of the 1 mol% orthorhombic (Fig. 7b,) and 0.1 mol% monoclinic (Fig. 7d,) samples we see that in the former the energy more efficiently leaks to the Eu^{2+} ions emitting at longer wavelengths. This points on a more efficient Eu(Sr1)→Eu(Sr2) energy transfer in the 1 mol% orthorhombic powder. This is reasonable, as in both phases the short-wavelength emission band overlaps partially with absorption (excitation) of the long-wavelength emitting centre. Thus energy from the more energetic luminescence centre of the Eu(Sr1) may be nonradiatively drained by the Förster mechanism [32] to the energetically lower levels of the Eu(Sr2). Thus, already the RT experiments prove that in both phases Eu^{2+} ions occupy the two available sites and give rise to distinct though partially overlapping emission bands. Below, we shall present low temperature experiments from which the presence of Eu^{2+} ions in different sites will be even more convincing.

Low temperature PLE and PL spectra of the Sr_2SiO_4:1 mol% Eu orthorhombic α'-phase (Fig. 8a,b- sample SEu8) and Sr_2SiO_4:0.1 mol% Eu monoclinic β-phase (Fig. 8c,d-sample SEu1) allowed for a more clear exposure of the two emitting centres in each phase. The α'-phase gives two clearly separated emitting bands peaking at 470 nm, Eu(Sr1), and 550 nm, Eu(Sr2), upon 310 nm excitation. The former gets relatively weaker with increasing excitation wavelength. When the excitation is performed at 400 nm or at yet lower energies only the longer wavelength emission band (550 nm) is present. Low-temperature PLE spectra show that the most efficient excitation of the long wavelength emission (peaking at 550 nm) occurs around 430 nm while the short wavelength luminescence (470 nm) is most effectively excited around 330 nm. In the excitation spectrum of the 550 nm luminescence (Eu(Sr2)), the bands characteristic for the other centre (Eu(Sr1)) are clearly present, though they have low intensities. It is clear that some Eu(Sr1)→Eu(Sr2) energy transfer occurs.

Therefore, it is not possible to record exclusively luminescence of the high energy, Eu(Sr1), centre. A long-wavelength excitation (460 nm) produces a single band emission (Fig. 8b, red line) which is slightly red-shifted and peaks around 600 nm. A closer inspection reveals that its shape is slightly distorted suggesting a superposition of two components. This is surprising as the host does not offer a third site. A possibility of a small admixture of the β-phase (not recordable by XRD) cannot explain this effect as the β-phase does not produce such a long-wavelength luminescence, as we shall see shortly. Excitation spectrum of the emission monitored at 620 nm indeed shows a noticeable long-wavelength broadening compared to the PLE of the 550 nm emission, see Fig. 8a. It is possible that certain Eu(Sr2) centres experience some structural distortion. Yet, details of this effect remain unclear at present. Note that the presented spectra are normalized to the same height. In fact the long-wavelength emission is much less intense than the two regular ones peaking around 475 nm and 550-560 nm.

In the case of the monoclinic β-phase (Sr_2SiO_4:0.1 mol% Eu), see Fig. 8c,d quite a similar behaviour at 30 K is observed. Two emission bands peaking at 470 nm (Eu(Sr1)) and 545 nm (Eu(Sr2)) are clearly seen. Again only the one at longer

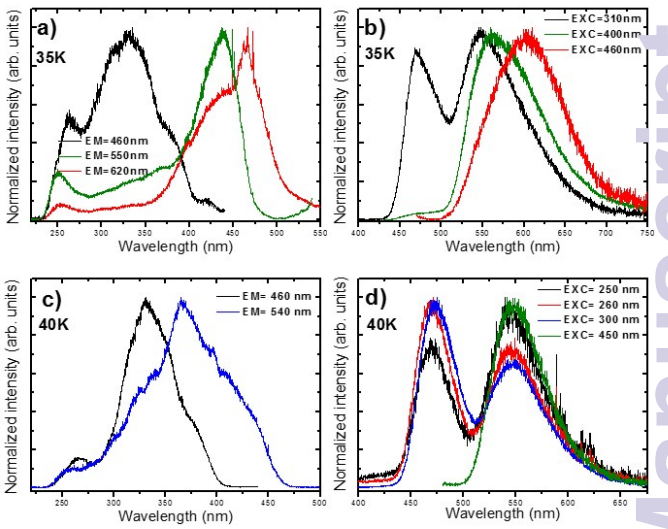

Fig.8.Low temperature excitation and emission spectra of the powders: a) and b) orthorhombic- Sr_2SiO_4: 1 mol% Eu (SEu8), c) and d) monoclinic- Sr_2SiO_4:0.1 mol% Eu (SEu1).

wavelength can be generated separately. The more energetic emission is always accompanied by the less energetic one due to the unavoidable energy transmission down to the Eu(Sr2) centre. PLE spectra of the Eu(Sr2) centre indeed contain features characteristic for the Eu(Sr1) one. Thus, the Eu(Sr1)→Eu(Sr2) energy transfer occurs also for the Sr_2SiO_4: 0.1 mol% Eu β-phase even for so low Eu content. The Eu(Sr2) centre may be exclusively excited in the 420-450 nm range of wavelengths, see Fig. 8c and 8d.

From Table 2 and the recorded crystallographic data we know that orthorhombic Eu-activated Sr_2SiO_4 powders can be fabricated both using H_3BO_3 or $SrCl_2$ flux if only the dopant content is not lower than 1 mol%. It is interesting to compare luminescence spectra of such two compositions upon excitation at 255 nm. This is presented in Fig. 9a (sample SEu8, SEu12). It is immediately evident that under such radiation the luminescence of the material made using H_3BO_3 flux contains quite a significant admixture of the Eu^{3+} emission superimposed on the Eu^{2+} band. In the case of the powder synthesized with the help of $SrCl_2$ flux the luminescence is generated by Eu^{2+} ions, exclusively. Thus, for some reasons, H_3BO_3 hinders the susceptibility for chemical reduction of Eu^{3+} to the Eu^{2+} form. At this point the reasons for that are not clear. Yet, in Fig. 9b (sample SEu8, SEu12), which present IR spectra of the orthorhombic versions of Sr_2SiO_4:Eu powders made with the help of both fluxes, we find information which seems to be useful in understanding this difference. Namely, in the case of the powder made using the H_3BO_3 flux in the 1150-1300 cm^{-1} range of wavenumbers two well-resolved components are clearly seen. They can be identified as resulting from B–O stretching vibrations [33]. Thus, boron enters the Sr_2SiO_4 host as an impurity. Since B^{3+} is a small ion (0.11 Å) it is expected to replace Si^{4+} (0.26Å), as all other sites are occupied by greater larger ions. If so, however, the smaller charge of B^{3+} compared

to Si^{4+} may easily stabilize the Eu^{3+} ions (in the position of Sr^{2+}) [34] as then the electrostatic neutrality is maintained.

Similar comparison for the monoclinic structure could not be done as with Eu activator it could not be obtained as a pure phase. Thus, we can conclude that, compared to H_3BO_3, $SrCl_2$ flux not only allows fabrication of powders with a better morphology but also facilitates reduction of Eu^{3+} to Eu^{2+}.

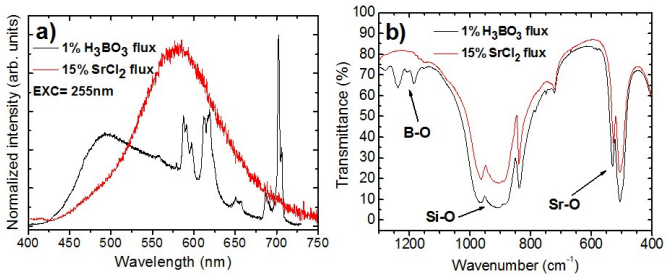

Fig.9.a)Comparison of luminescence spectra of α'-Sr_2SiO_4: 1 mol% Eu obtained in the synthesis with fluxes- H_3BO_3(sample SEu12- black line) and $SrCl_2$ (sample SEu8- red line) upon excitation at 255 nm b) Infrared spectra of α'-Sr_2SiO_4: 1 mol% Eu obtained in the synthesis with fluxes- H_3BO_3(sample SEu12- black line) and $SrCl_2$ (sample SEu8- red line).

Radioluminescence

Independently on its crystal structure, Sr_2SiO_4 is not a dense material (~5 g/cm^3), and thus it is not very attractive host for scintillation applications. Yet, we present radioluminescence (RL) spectra for both phases of Sr_2SiO_4:Ce (Fig. 10- sample SCe15, SCe26) and Sr_2SiO_4:Eu (Fig. 11- sample SEu1, SEu8) as they appear quite intriguing.

The striking differences are observed between the orthorhombic and monoclinic Sr_2SiO_4:Ce materials in both the spectral distribution of the RL emissions and their efficiencies. The orthorhombic Sr_2SiO_4:Ce α'-phase (Fig. 10, blue line) gives only a weak emission upon excitation with X-rays, at the level of ~10% of the commercial Lu_2SiO_5:Ce (LSO). Furthermore, the RL spectrum covers much broader range of wavelengths (~375-650 nm) than it was seen in PL (see Fig. 5b and 6b). Upon optical excitation the spectra of this phase were much narrower which may imply that the inefficient RL results from both Ce and a defect/defects generated upon the impact of the high energy X-rays. In contrary, the RL of the monoclinic Sr_2SiO_4:Ce β-phase (Fig. 10, red line) gives emission whose efficiency at least meets, if not surpasses, the yield of LSO. It cannot be excluded that the already impressive RL of the monoclinic Sr_2SiO_4:Ce might be further improved if dopant content and processing parameters are further optimized. This was beyond the scope of the present research, however. Since in photoluminescence such drastic differences in intensities of the emissions from the two phases were definitely not seen (though quantitative measurements were not performed) we may conclude that in the orthorhombic α'-phase the efficiency of the host-to-activator energy transfer is critically lower, than in the case of the monoclinic β-phase [35].

Also RL spectra of the Sr_2SiO_4:Eu presented in Fig. 11 surprise to some extent. In this case Eu^{2+} gives quite significant RL from both phases. Yet, it appears that, in contrast with PL presented

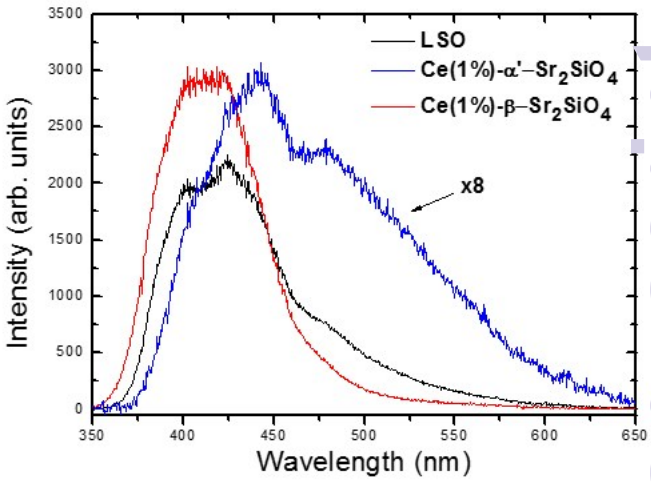

Fig.10. Radioluminescence spectra of Sr_2SiO_4:1 mol% Ce obtained in the synthesis with flux 1wt% H_3BO_3 (blue line- orthorhombic phase, sample SCe26) and 50w $SrCl_2$ (red line, monoclinic phase, sample SCe15) at 1400°C 4h in air.

in Fig.7b and 7d in both polymorphs only the Eu(Sr2), luminescent centre is active in generation of light. It appears that the energy transfer from the host excited upon the impact of X-rays is preferentially transferred to the Eu^{2+} ions giving th long-wavelength luminescent band peaking around 580 nm in the orthorhombic phase and around 540 nm in the monoclinic one (5-10 nm shift between peaks in RL and PL may results from the fact that the former spectra were not corrected for the system characteristics). The reason of such behaviour is not clear at present and its explanation would require rather extensive, specialized research. Yet, a reasonable explanation/guess might be that the Eu(Sr2) ions giving the long-wavelength luminescence are more efficient hole-tra

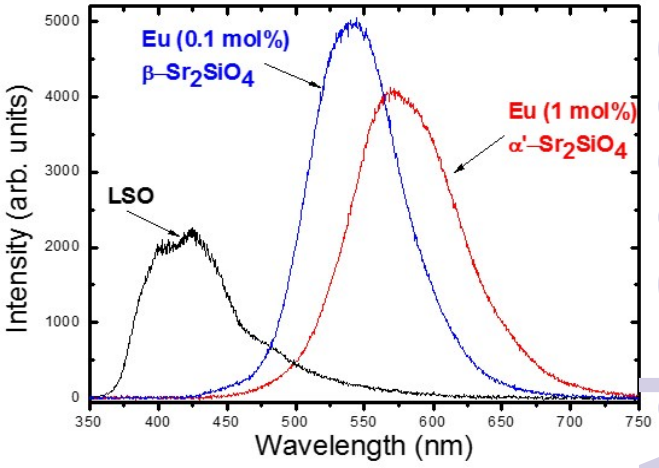

Fig.11. Radioluminescence spectra of Sr_2SiO_4: x mol% Eu (x=0.1, 1 mol%) obtained in the synthesis with 15wt% of $SrCl_2$ flux at 1400°C 4h in active carbon atmosphere. Sample SEu1 (blue line) crystallizes in monoclinic phase, while SEu8 (red line) orthorhombic.

compared to Eu(Sr1). Such a preferential trapping of holes by Eu(Sr2) would automatically make these ions more attracti e for subsequent trapping of electrons from the conduction band, which would close the first step of harvesting the energy fro n

excited host by the emitting centres [36-38]. Consequently, only the Eu(Sr2) centre would be fed by the energy acquired from the incident X-ray photons and only these ions would produce luminescent photons. A strongly preferential transfer of energy from a host to a dopant located in a specific symmetry site is a known effect. For example in Lu_2SiO_5:Ce (LSO) scintillator crystals used in positron emitting tomography (PET) cameras also, for lower concentrations, only one Ce site gives light upon the impact of γ-rays [39].

Conclusion

Fabrication conditions of phase pure monoclinic powders of Sr_2SiO_4, monoclinic and orthorhombic $Sr_2SiO_4:Ce^{3+}$ as well as monoclinic and orthorhombic $Sr_2SiO_4:Eu^{2+}$ were established using H_3BO_3 or $SrCl_2$ fluxes. It was showed that both the flux used in the fabrication process as well as the type and concentration of the activator affect the crystallization process and defines the type of structure formed. The single phase powders of both phases activated with Ce^{3+} or Eu^{2+} were spectroscopically investigated at 30 K and 300 K. In both polymorphs the dopants were showed to occupy two symmetry sites. Their emission and excitation spectra were recorded at 30 K and 300 K and it was showed that ions emitting at shorter wavelengths transfer energy to those producing luminescence at longer wavelengths. This effect was especially significant at room temperature. For a specific activator the emissions locates at quite similar range of wavelengths for both polymorphs. In the case of Ce^{3+} the luminescence bands of both sites locates partially in the UV part of spectrum and efficient excitation is possible below ~360 nm. Such characteristics is problematic if application of this composition in solid state lighting is considered. Eu^{2+} produces emission bands which locate fully in visible region. At room temperature, excitation with blue LED (~450 nm) give rise to broad green luminescence in the monoclinic phase of Sr_2SiO_4:Eu and orange emission in the orthorhombic form. Efficient emission from both Eu^{2+} sites simultaneously can be achieved upon excitation around 375-400 nm for the monoclinic structure.

Acknowledgements

The work was supported by Wroclaw Research Centre EIT+ within the project "The Application of Nanotechnology in Advanced Materials" - NanoMat (POIG.01.01.02-02-002/08) co-financed by the European Regional Development Fund (Innovative Economy Operational Program 1.1.2).

References

1 X. Sun, J. Zhang, X. Zhang, Y. Luo, X. Wang, Journal of Rare Earths **26(3**), (2008), 421
2 L. Pan-Li, Y. Zhi-Ping, W. Zhi-Jun, G. Qing-Lin, Chinese Physics B **17(3**), (2008), 1135
3 S.K. Gupta, M. Moharpatra, S. Kaity, V. Natarajan, S.V. Godbole, Journal of Luminescence **132**, (2012), 1329
4 Y. Qiao, X. Zhang, X. Ye, Y. Chen, H. Guo, Journal of Rare Earths **27(2)**, (2009), 323
5 J.H. Lee, Y.J. Kim, Journal of Ceramics Processing Research **10 (1)**, (2009), 81
6 D.V. Sunitha, H. Nagabhushana, S.C. Sharma, B.M. Nagabhushana, B. Daruka Prasad, R.P.S. Chakradhar, Spectrochimica Acta Part A: Molecular and Biomolecular Spectroscopy **127** (2014) 381-387
7 W. Qi, Q. Jian-Bei, S. Zhi-Guo, Z. Da-Cheng, X. Xu-Hui, Chinese Physics B **23(6)**, (2014), 064211-1
8 H. Nagabhushana, D.V. Sunitha, S.C. Sharma, B. Daruka Prasad, B.M. Nagabhushana, R.P.S. Chakradhar, Journal of Alloys and Compounds **595** (2014) 192
9 M.A. Tshabalala, F.B. Dejene, S.S. Pitale, H.C. Swart, O.M. Ntwaeaborwa, Physica B **439** (2014), 126
10 L.Ch. Ju, X. Xu, L.Y. Hao, Y. Lin, M.H. Lee, Journal of Materials Chemistry C **3** (2015), 1567
11 B. Zhang, X. Yu, T. Wang, S. Cheng, J. Qiu, X. Xu, Journal of American Ceramic Society **98 (1)**, (2015), 171
12 J. Barzowska, A. Chruścińska, K. Przegiętka, K. Szczodrowski, Radiation Physics an Chemistry **104** (2014) 31
13 N. Lakshminarasimhan, U.V. Varadaju, Materials Research Bulletin **43**, (2008), 2946
14 Z. Song, X. Ding, S. Yang, F. Du, L. Bian, S, Duan, Q.L. Liu, Journal of Luminescence **152** (2014), 199
15 X. Xu, X. Zhang, T. Wang, J. Qiu, X. Yu, Materials Letters **127** (2014)40
16 S.H. Lee, H. Y. Koo, Y.Ch. Kang, Ceramics International **36** (2010), 1233
17 Ch-H. Hsu, R. Jagannathan, Ch.H. Lu, Materials Science and Engineering B **167**, (2010), 137
18 J.K. Han, M.E. Hannah, A. Piquette, G.A. Harita, J.B. Talbot, K.C. Mishra, J. McKittrick, Journal of Luminescence **132**, (2012), 106
19 D. Dutczak, A. Milbrat, A. Katelnikovas, A. Meijerink, C. Ronda, T. Jüstel, Journal of Luminescence **132**, (2012), 2398
20 R.Y. Yang, H.Y. Chen, S.J. Chang, Y.K. Yang, Journal of Luminescence **132**, (2012), 780
21 L. Zhang, Z. Lu, P. Han, J. Lu, N. Xu, L. Wang, Q. Zhang, Journal of American Ceramic Society **95 (12**), (2012), 3871
22 L. Zhang, P. Han, K. Wang, Z. Lu, L. Wang, Y. Zhu, Q. Zhang, Journal of Alloys and Compounds **541** (2012) 54
23 L.CH. Ju, Ch. Cao, Q.Q. Zhu, J.Y. Tang, L.Y. Hao, X. Xu, Journal of Materials Science: Materials in Electronics **24** (2013), 4516
24 H. Feng, Y. Yang, X. Zhang, Y. Xu, J. Guan, Superlattices and Microstructures **78**, (2015), 150
25 M.A. Tshabalala, H.C. Swart, O.M. Ntwaeaborwa, Journal of Vacuum Science & Technology A **32**, (2014), 021401
26 M. Pardha Saradhi, N. Lakshminarasimhan, S. Boudin, K. Vijay Kumar Gupta, U.V. Varadaraju, B. Raveau, Materials Letters **117**, (2014), 302
27 M. Catti, G. Gazzonni, G. Ivaldi, G. Zanini, Acta Crystallographica **B 39**, (1983), 674
28 M. Catti, G. Gazzonni, Acta Crystallographica **B 39**, (1983) 679
29 M. Catti, G. Gazzonni, G. Ivaldi, Acta Crystallographica **C 39** (1983),29
30 M. Catti, G. Gazzonni, G. Ivaldi, Acta Crystallographica **B 40**, (1984),537

31 J. Liu, Ch.G. Duan, W.N. Mei, J.R. Hardy, Journal of Chemical Physics **116(9)**, (2002), 3864

32 T. Förster, Annalen der Physik **2**, (1948), 55

33 R.D. Shannon; Acta Cryst. **A 32**, (1976), 751.

34 F.A. Miller, C.H. Wilkins ; Anal. Chem. **24(8)**, 1952, 1253

35 E.Zych Luminescence and scintillation of inorganic phosphor materials. In: Handbook of Luminescence, Display Materials, and Devices. Vol. 2. Inorganic Display Materials, ed. by Hari Singh Nalwa, Lauren Shea Rohwer. - Stevenson Ranch, Calif., 2003., American Scientific Publishers 2003, 251

36 A.J. Wojtowicz, A. Lempicki, D. Wisniewski, M. Balcerzyk, C Brecher, IEEE Transactions on Nuclear Science **43(3)**, (1996), 2168

37 E. Zych Nanocrystalline insulating phosphors in: Doped nanomaterials and nanodevices Vol.1. Luminescence and applications/ ed. By W. Chen, Stevenson Ranch American Scientific Publisher, 2010, 14335

38 A. Lempicki, A.J.Wojtowicz, C. Brecher Inorganic Scintillators in Wide-Gap Luminescent Materials: Theory and Applications/ ed. S.R. Rotman, Kluwer Academic Publishers, Inc., Norwell MA, USA. 1997, 235

39 A. Vedda, M. Nikl, M. Fasoli, E. Mihokova, J. Pejchal, M. Dusek, G. Ren, C.R. Stanek, K.J. McClellan, D.D. Byler, Physical Review B **78**, (2008), 195123